

# Outflow of Gas from Supersonic Nozzle with Screen into Vacuum

J.C. Lengrand<sup>a</sup>, V.G. Prikhodko<sup>b</sup>, P.A. Skovorodko<sup>b</sup>,  
I.V. Yarygin<sup>b</sup> and V.N. Yarygin<sup>b</sup>

<sup>a</sup>CNRS/ICARE, 1C av. de la recherche scientifique, 45071 Orléans Cedex 2, France

<sup>b</sup>Institute of Thermophysics SB RAS, 630090, Novosibirsk, Russia

**Abstract.** The outflow of gas into a vacuum from a supersonic nozzle with a screen mounted at the nozzle exit has been investigated both experimentally and numerically. The level of back flux was estimated by the pressure inside the probe placed in the backflow region. The obtained results indicate a possibility to decrease the back flux by putting a screen on the exit part of the nozzle, though improper screen geometry may cause even the back flux to increase.

**Keywords:** Outflow into vacuum, supersonic nozzle, free jet, screen, backflow region, back flux, simulation, DSMC

**PACS:** 02.70.Uu, 05.10.Ln, 47.10.ad, 47.11.Bc, 47.40.Ki, 47.45.-n, 47.60.Kz

## INTRODUCTION

When a gas exits from a sonic or supersonic nozzle into vacuum, the limiting angle  $\theta_{\max}$  of jet expansion exceeds  $90^\circ$  relative to the nozzle axis. The flow of gas at angles  $\theta > 90^\circ$  is known as *backflow*. Such flows arise when operating orientation and control thrusters of space vehicles, in the operation of high-vacuum jet pumps, and also in a number of vacuum technological devices. As a rule, backflow has a negative character and should be minimized.

Backflow control by means of special gas dynamic protecting devices (screens) mounted at the exit of the nozzle is discussed in the paper. This study is a continuation of paper [1] where the flow inside the screen was studied both experimentally and numerically. Up to now the problem of reducing gas phase backflow by means of screens was not practically considered.

## THE EXPERIMENTAL SET-UP AND DIAGNOSTIC ITEMS

Experiments were carried out on the large-scale vacuum gas dynamic facility VIKING of the Institute of Thermophysics (Siberian Branch of the Russian Academy of Sciences), whose detailed description is presented in [2]. The difficulties for an experimental investigation of backflows are related to the necessity of a very low pressure in the ambient space around a source of gas and, accordingly, to have a high sensitivity equipment allowing to perform measurements in a rarefied gas. VIKING allows to generate a supersonic flow with a large gas flow rate and to have a high vacuum in the working chamber either in steady conditions (with use of rather expensive cryogenic pumping) or in pulsed mode (cheap alternative). The reported experiments were carried out under a pulsed mode with pulse times up to 1 s. The intensity of backflow was estimated from the value of the total pressure in the corresponding points of space.

In experiments a conical supersonic nozzle was used, with half-angle  $14.2^\circ$ , throat diameter  $d_* = 10$  mm and exit diameter  $d_a = 20$  mm (geometrical exit Mach number  $M = 2.94$ ). The nozzle was associated to replaceable screens of different heights. The ratio between screen and nozzle diameters was  $d_s/d_a = 1.75$ . The relative disposition of nozzle, screen and total pressure probe is shown in Fig. 1. Screens have been selected so that the angle  $\alpha$  between a straight line connecting internal edges of nozzle and screen and the nozzle centerline varied from  $30^\circ$  to  $90^\circ$ . As a quick-response gauge of total pressure an ion gauge head PMI-10-2 was used and could be considered as a Pitot tube.

At the front end of the gauge a slot-hole mouthpiece of size  $3.5 \times 29$  mm was tightly fastened. The radius of the inlet part of the pressure probe was 36 mm. The mouthpiece limited the area of registration of back streams up to  $94^\circ \leq \varphi \leq 106^\circ$  for the nozzle with screen, increased approximately the signal by a factor of 2 and, that is very important, reduced the influence on probe readings of the growing pressure in the working chamber during nozzle operation. Due to geometrical reasons the range of streamline angles for the flow entering the probe inlet was  $93^\circ \leq \varphi \leq 101^\circ$  for the nozzle without screen.

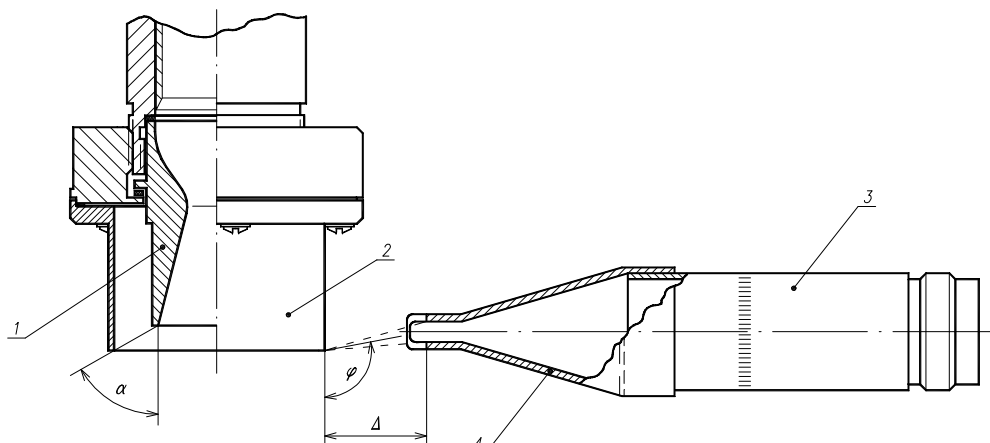


**FIGURE 1.** Scheme of working part. 1 – supersonic nozzle, 2 – screen, 3 – pressure gauge PMI-10-2, 4 – slot-hole mouth-piece.

All experiments were done at room temperature. Before nozzle gas feeding, the working chamber was pumped down to a pressure  $\leq 10^{-3}$  Torr. The working gas (Air) was fed from a compressor through a buffer vessel consisting of 4 standard 40-liters tanks. Registration of backflow was carried out right after the formation of a gas jet while the pressure growth in the working chamber did not disturb the streamlines in the backflow region and the background gas did not start to get into the pressure gauge.

During the experiment the following parameters were measured: pressure of compressed air in the supplying pipeline, pressure of gas in the nozzle stagnation chamber, ambient pressure in the vacuum chamber and readings of the total pressure probe. The scheme of measurements is shown in Fig. 2.

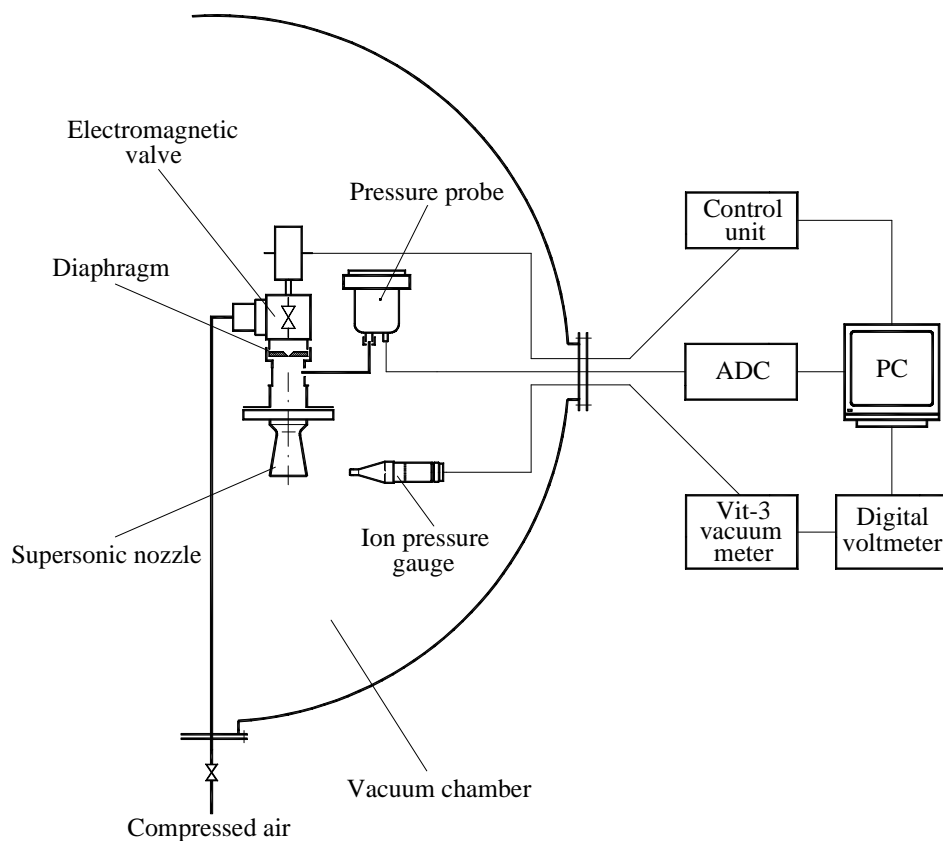


**FIGURE 2.** Scheme of measurements.

The gas pressure in the nozzle stagnation chamber was adjusted in a range 75–792 Torr and registered by an abso-

lute pressure gauge IKD-6TDA whose signal was moved to a 12 digit ADC and further to the computer. Initial and final pressures in the working chamber were registered by a capacitive gauge Baratron 626A with full-scale of 0.1 Torr. To know how the ambient pressure in the space near the nozzle varies during gas expansion from the nozzle separate experiments have been made. For this purpose in front of the Pitot tube at a distance  $\approx 4$  mm from inlet slot edges, a flat screen of size  $46 \times 19$  mm was mounted intercepting a direct stream of air to the sensor, and the measured pressure behind the screen was assumed to be the value of the background pressure.

The gauge PMI-10-2 measuring a backflow of gas was connected to a vacuum meter VIT-3, which provided power supply of the gauge and initial amplification of ion current. After amplification the signal was transferred to the input of a digital voltmeter AVM-4306 connected to a computer through a RS-232 interface. The same computer controlled the electromagnetic valve which injected gas into the nozzle. The developed software allowed operating synchronously nozzle flow and recording of measured signals. After each experiment all chain of total pressure measurements equipment was calibrated in static conditions with a known pressure measured by Baratron.

The experiments were performed for three values of initial stagnation pressure  $p_0$ : 75 Torr, 270 Torr and 792 Torr, and 3 variants of screen geometry with angles  $\alpha$  of  $30^\circ$ ,  $45^\circ$ , and  $90^\circ$  in addition to the experiment for a nozzle without screen. The total number of studied regimes was therefore 12. The results obtained for  $p_0 = 270$  Torr are illustrated in Fig. 3 where the time dependence of the ratio of the measured total pressure to the current pressure in the stagnation chamber is presented. The command for opening gas supply to stagnation chamber was given by the computer at time  $t = 0.5$  s. A delay of approximately 0.1 s is due to inertia of the electromagnetic valve.

It is possible to see that a rather quick (about 0.1 s) nozzle start takes place. Then during 0.2 s the readings of the pressure probe are nearly constant. Throughout the duration of a short pulse the ambient gas has not enough time to affect the measured pressure.

The presented results illustrate that screens do have a significant influence on backflow. The most interesting is the fact that this influence is not monotonous – the screens with angles  $90^\circ$  and  $45^\circ$  reduce backflow. However for the screen with angle  $30^\circ$  the backflow could be larger or smaller than for a nozzle without screen depending on the stagnation pressure. This conclusion is important for practical applications and the probable reason of this effect will be discussed below in the comparison of the obtained experimental data with the results of calculations.

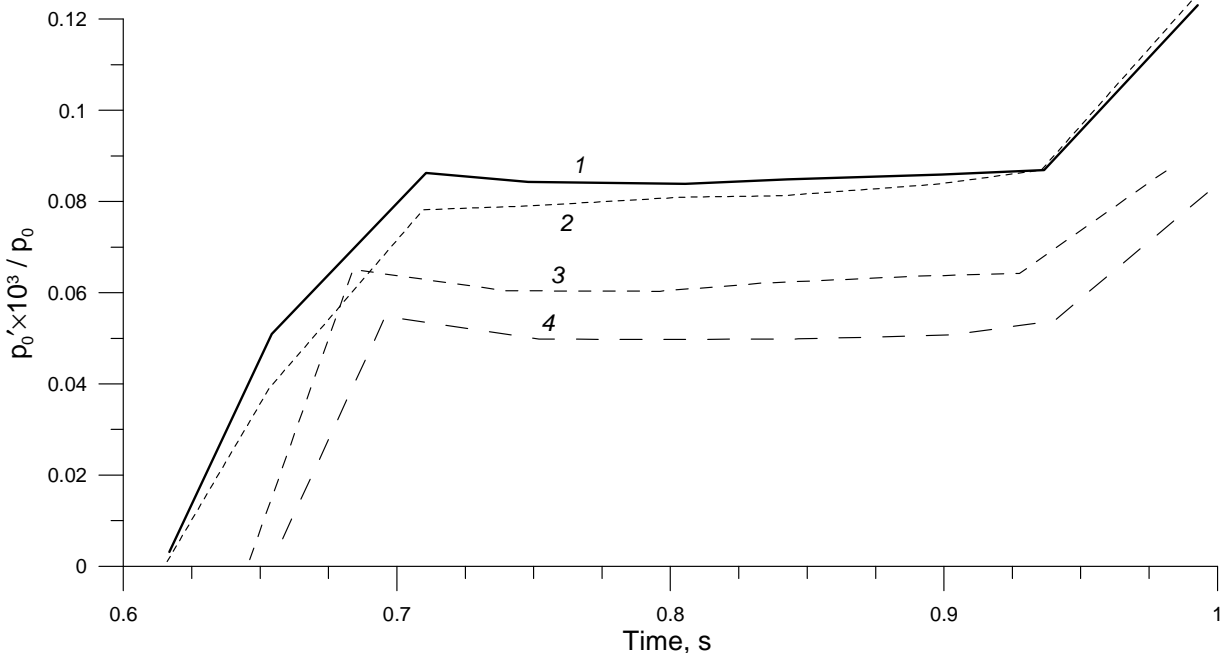


**FIGURE 3.** Ratio of total pressure to stagnation chamber pressure for regime with  $p_0 = 270$  Torr .  
 1 – nozzle without screen, 2 – nozzle with  $30^\circ$  screen, 3 – nozzle with  $45^\circ$  screen, 4 – nozzle with  $90^\circ$  screen.

## NUMERICAL SIMULATION OF THE FLOW

The simulation of the flow inside the screen volume at experimental conditions was performed using the full set of unsteady Navier-Stokes (NS) equations, that were solved numerically by an original algorithm based on a staggered grid (NS – algorithm) [3]. The domain of simulation consisted of two rectangular regions, as shown by dashed lines in Fig. 4. The distribution of parameters in the nozzle exit section that was used as one of the boundary conditions was obtained by a preliminary calculation based on parabolized Navier-Stokes (PNS) equations, that were solved by a marching procedure (PNS – algorithm) [4]. This calculation was performed using 25 streamtubes, the flow in the throat

section was assumed to be sonic and uniform. Here and below the solid wall temperature  $T_w$  was assumed to be equal to the stagnation temperature  $T_0$ . The air was assumed to be a perfect gas with specific heats ratio  $\kappa = 1.4$ . The temperature dependence of the dynamic viscosity of air was taken for a Lennard-Jones (6 – 12) potential with parameters  $\sigma = 3.617 \text{ \AA}$ ,  $\varepsilon/k = 97 \text{ K}$ . The Prandtl number  $Pr$  was assumed to be constant and equal to 0.71. The simulations were performed for typical values of stagnation parameters:  $T_0 = 293 \text{ K}$ ,  $p_0 = 75 \text{ Torr}$ ,  $270 \text{ Torr}$  and  $792 \text{ Torr}$ . The Reynolds numbers  $Re$  based on the conditions in the nozzle throat section and its radius for the considered regimes were equal to 7501, 27004 and 79213, respectively. In spite of rather large values of the Reynolds numbers the simulated flow was assumed to be steady, axisymmetric and laminar.

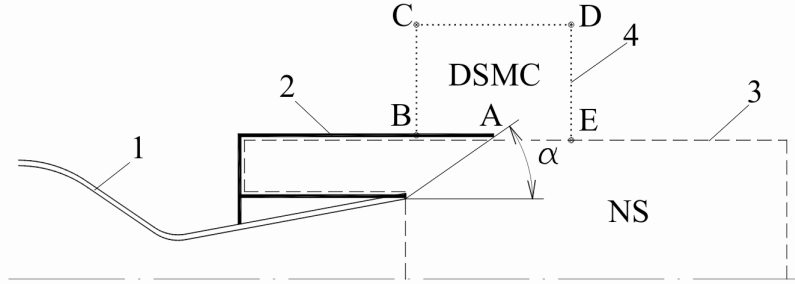


**FIGURE 4.** Scheme of the nozzle with the screen. 1 – nozzle, 2 – screen, 3 – border of the domain of simulation for NS – algorithm, 4 – border of the domain of simulation for DSMC – algorithm.

The simulation of the flow in the domain shown in Fig. 4 by dashed lines was performed on a uniform rectangular grid with mesh sizes  $dr = dx = 0.05 \text{ mm}$ . The axial coordinate  $x$  is counted from the position of the screen bottom, the nozzle exit section being located at  $x = 20.4 \text{ mm}$ , while the right boundary of the domain is located at  $x = 100 \text{ mm}$ . The radial size of the domain is  $17.5 \text{ mm}$ . The internal radius of the domain in the nozzle region is  $11 \text{ mm}$  that is  $1 \text{ mm}$  larger than the nozzle exit radius, which corresponds to the thickness of the nozzle lip ( $h_{lip} = 1 \text{ mm}$ ).

The conditions at nozzle exit and flow axis of the domain were stated as usual [3]. On solid surfaces the velocity slip and temperature jump were taken into account assuming full accommodation. The parameters on the output boundaries were found by interpolation from internal points of the domain according to the conditions of a supersonic flow without any upstream disturbances. The simulations were performed for 3 values of angle  $\alpha$ :  $30^\circ$ ,  $45^\circ$  and  $90^\circ$ .

In our previous paper [1] devoted to the analysis of the same experiment performed for  $p_0 = 900 \text{ Torr}$ , the flow behind the screen was simulated by two approaches, namely the Direct Simulation Monte Carlo (DSMC) method [5] (PNS-NS-DSMC approach) and the above-mentioned PNS algorithm (PNS-NS-PNS approach) since PNS algorithm was found to be an efficient one to describe the peripheral part of the jet issuing into vacuum [6, 7]. As it was found in [1] both mentioned approaches predict similar results for the values of the back fluxes for all the screens with  $30^\circ \leq \alpha \leq 90^\circ$ . That is why in this study only PNS-NS-DSMC approach was used to describe the flow behind the screen.

The rectangular domain ABCDE of simulation of the flow by a DSMC-algorithm is schematically shown in Fig 4. The emission of molecules in the domain was performed radially through the surface AE based on the distribution of parameters obtained earlier by the NS-algorithm. On surfaces BC, CD and DE full absorption of incident molecules was assumed. The solid surface AB was assumed to be diffusely or specularly reflecting. The collisional properties of molecules were described by the VSS molecular model for a repulsive interaction potential between molecules ( $\omega = 0.75$ ,  $\alpha_{VSS} = 1.5325$ ) [5]. To take into account the effect of rotational degrees of freedom of molecules the known Larsen-Borgnakke procedure [5] was applied. The simulations were performed for the value of the rotational collision number  $Z_r = 5$ . Since the main problem solved by DSMC simulation is the distribution of parameters in the backflow region ( $\theta > 90^\circ$ ) the axial and radial dimensions of the domain ABCDE were chosen to provide acceptable accuracy for that considered part of the flow. Through a series of test-calculations these optimal dimensions were found to be:  $BA = AE = 10 \text{ mm}$ ,  $BC = 20 \text{ mm}$  for the regime with screen and  $BA = AE = 10 \text{ mm}$ ,  $BC = 30 \text{ mm}$  for the regime without screen. Outside domain BCDE the flow was assumed to be collisionless. To collect the asymptotic properties of the flow at infinitely large distances from the device the properties of individual molecules leaving the domain through surfaces BC and CD were sampled with weighting factor  $1/v$ , where  $v$  is the absolute value of molecule velocity. The simulations were performed during  $2 \cdot 10^4$  time steps with  $10^6 \div 3 \cdot 10^6$  simulated molecules at the steady stage.

To calculate the backflow region for the case without a screen the domain ABCDE was moved to the nozzle in such a way that the point A was placed in the nozzle exit section at  $r = 11 \text{ mm}$  ( $h_{lip} = 1 \text{ mm}$ ). The distribution of parameters on the starting surface AE for this case was estimated based on the results of simulation the flow inside the screen with  $\alpha = 90^\circ$  by NS-algorithm. This regime is characterized by minimum value of base pressure [1] with minimum deviations of the parameters on the surface AE from those taking place at expansion of gas into vacuum from the nozzle without screen.

## RESULTS AND DISCUSSION

Since the asymptotic properties of the flow at large distances  $R$  from the device were illustrated in detail in paper [1], only the numerical results for the values measured in our experiments will be reported here.

For the measured values of pressure in the probe the mean free path of molecules inside the probe lies in the range  $1.3 \div 8.6$  mm. The corresponding Knudsen number over the slot width 3.5 mm lies in the range  $0.37 \div 2.5$ . The regime of gas flow inside the probe is close, therefore, to free molecular. In this case the readings of the probe should be completely determined by the flow rate of gas incoming inside the probe through the probe slot. During DSMC simulation this flow rate through the control surface corresponding to the position of the probe slot was collected thus allowing the calculation of the absolute value of the pressure inside the probe.

All the obtained experimental and theoretical data concerning the dependence of pressure inside the probe on the angle of screen  $\alpha$  for the regimes with  $p_0 = 75$  Torr, 270 Torr and 792 Torr are presented in Figs. 5-7, respectively. The data for nozzle without screen are also shown for comparison.

As it is seen from these figures, the measured and predicted values of absolute values of pressure inside the probe are in good agreement. Maximum effect of the screen towards reducing the value of back flux takes place for the screen with  $\alpha = 90^\circ$  for all considered values of stagnation pressure.

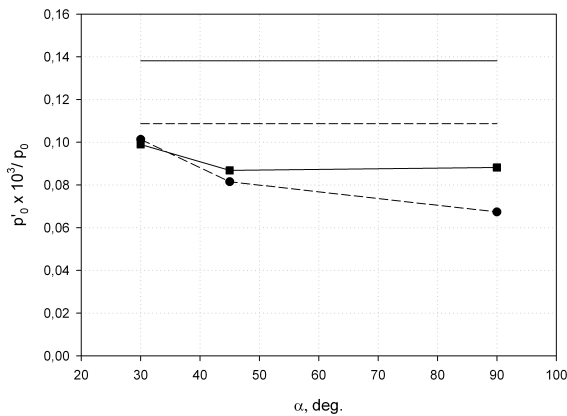


**FIGURE 5.** Measured (solid lines and squares) and numerical (dashed lines and circles) data for normalized probe pressure for the regime with  $p_0 = 75$  Torr for studied screens. The data for nozzle without screen are shown by lines without symbols.

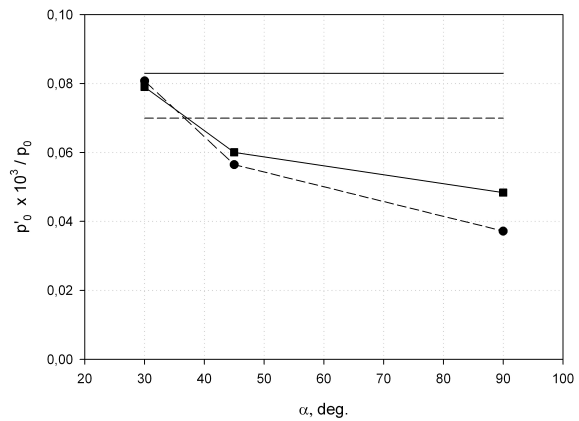


**FIGURE 6.** Measured (solid lines and squares) and numerical (dashed lines and circles) data for normalized probe pressure for the regime with  $p_0 = 270$  Torr for studied screens. The data for nozzle without screen are shown by lines without symbols.

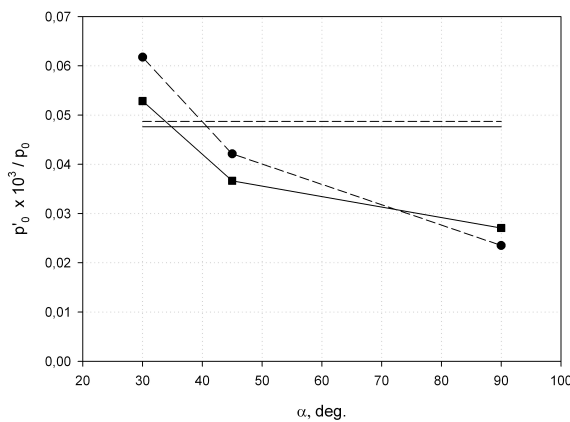


**FIGURE 7.** Measured (solid lines and squares) and numerical (dashed lines and circles) data for normalized probe pressure for the regime with  $p_0 = 792$  Torr for studied screens. The data for nozzle without screen are shown by lines without symbols.

For the regime with  $p_0 = 75$  Torr all the considered screens allow reducing the back flux compared with the case of nozzle without screen.

For the regime with  $p_0 = 270$  Torr the situation is ambiguous: theory predicts small increase of back flux for the screen with  $\alpha = 30^\circ$  compared with the case of a nozzle without screen while the experiments did not confirm this result.

For the regime with  $p_0 = 792$  Torr both experiment and theory reveal the increase of back flux for the screen with  $\alpha = 30^\circ$  that means that improper screen geometry may cause even the back flux to increase.

## CONCLUSION

The main results of the performed study may be summarized as follows:

1. It is possible to decrease the back flux (by factor of about two in the considered conditions and geometry) by putting a screen on the exit part of the nozzle, though improper screen geometry may cause even the back flux to increase.
2. Maximum effect of the screen towards reducing the value of back flux takes place for the screen with  $\alpha = 90^\circ$  for all considered values of stagnation pressure.
3. Both experiment and theory reveal increasing of normalized back fluxes with decreasing the stagnation pressure or the Reynolds number.
4. The numerical data for absolute value of the pressure inside the probe placed in the backflow region are in good agreement with the measured results, which proves that the description of that region of the flow by the applied PNS-NS-DSMC approach is quite adequate.

## ACKNOWLEDGMENTS

This study was supported by the Russian Foundation for Basic Research (grant No.06-01-22004-CNRS).

## REFERENCES

1. J.C. Lengrand, V.G. Prikhodko, P.A. Skovorodko, I.V. Yarygin, and V.N. Yarygin, "Outflow of Gas from Nozzle with Screen into Vacuum," in *Rarefied Gas Dynamics: 26<sup>th</sup> International Symposium*, edited by T. Abe, AIP Conference Proceedings 1084, American Institute of Physics, Melville, NY, 2009, pp. 1158-1163.
2. V.G. Prikhodko, G.A. Khramov, and V.N. Yarygin, *Instruments and Experimental Techniques*, **39**, 2, 309-311 (1996).
3. A. Broc, S. De Benedictis, G. Dilecce, M. Vigliotti, R.G. Sharafutdinov and P.A. Skovorodko, *J. Fluid Mech.* **500**, 211-237 (2004).
4. P.A. Skovorodko, *Matematicheskoye modelirovaniye* **15**, 6, 95-100 (2003) (in Russian).
5. G.A. Bird, *Molecular Gas Dynamics and the Direct Simulation of Gas Flows*, Oxford, Clarendon Press, 1994.
6. P.A. Skovorodko, "Nonequilibrium Flow of Gas Mixture in Supersonic Nozzle and in Free Jet behind It," in *Rarefied Gas Dynamics: 20<sup>th</sup> International Symposium*, edited by Ching Shen, Beijing, Peking University Press, 1997, pp. 579-584.
7. J.C. Lengrand, J. Allegre, D. Bish, and P.A. Skovorodko, "Impingement of a Simulated Rocket Exhaust Plume onto a Surface," *Ibid.*, pp. 537-542.